Journal of The Electrochemical Society, **163** (3) Y5-Y11 (2016) Y5
0013-4651/2016/163(3)/Y5/7/$33.00 © The Electrochemical Society

Response to "Comment on Nanometer-Scale Corrosion of Copper in De-Aerated Deionized Water" [*J. Electrochem. Soc.*, 161, C107 (2014)]

Christopher Cleveland,[a] Mark E. Orazem,[a,*,z] and Saeed Moghaddam[b]

[a]*Department of Chemical Engineering, University of Florida, Gainesville, Florida 32611, USA*
[b]*Department of Mechanical and Aerospace Engineering, University of Florida, Gainesville, Florida 32611, USA*

This response is provided to comments by Spahiu and Puigdomenech criticizing the conclusion of Cleveland et al. [*J. Electrochem. Soc.*, **161**, C107 (2014)] that, in the absence of hydrogen, copper will corrode in deaerated deionized water. Spahiu and Puigdomenech base their critique on anomalies in the Pourbaix diagram presented by Cleveland et al., on concerns that the experimental system was inadequately deaerated, and on differences between the corrosion rates predicted in our work and in the work of Hultquist et al. [*Proceedings of the 2008 International Corrosion Congress*, Paper 3884, p. 1 (2008)]. In the present work, explanations are provided supporting our thermodynamic analysis and the experimental results. New numerical simulations show that the difference in estimated corrosion rates between our system and that published by Hultquist et al. are the natural consequence of scale and transport differences between the two systems. Thus, the comment that the difference in estimated corrosion rates between our system and that of Hultquist somehow invalidates our results is without basis. The concerns raised by Spahiu and Puigdoimenech do not invalidate the conclusions presented in Cleveland et al.

Manuscript received November 17, 2015. Published December 10, 2015.

In their Comment on Nanometer-scale corrosion of copper in de-aerated deionized water [*J. Electrochem. Soc.*, 161, C107 (2014)], Spahiu and Puigdomenech raise three principal objections:

1. Figure 5 in Cleveland et al.[1] does not properly represent the dependence of line "b" on the partial pressure of oxygen. In addition, the middle redox potential (ORP) presented in Figure 5 differs from the value calculated by Spahiu and Puigdomenech;
2. Spahiu and Puigdomenech suggest that trace amounts of oxygen in the experiment may be sufficient to explain the derived corrosion rates from the experiments performed;
3. Spahiu and Puigdomenech express concern that the observed corrosion rate by Cleveland et al.[1] is around three orders of magnitude higher than the rate that may be derived from the observations published by Hultquist et al.[2,3]

From these criticisms, Spahiu and Puigdomenech posit that our work[1] "may not be considered to support the claim that copper will corrode in deaerated deionized water if hydrogen is removed." Our response to these critiques are presented below.

Thermodynamic Analysis

Spahiu and Puigdomenech are correct to observe that line (b) shown in Figure 5 of our work does not properly represent the three cases discussed. Our presentation of a single Pourbaix diagram with three oxidation/reduction potentials overlaid was intended to show that copper is stable in anoxic water in the presence of hydrogen but has a tendency to corrode in water containing oxygen or in anoxic water that is free of hydrogen. We agree that presentation of three Pourbaix diagrams would have lessened cause for confusion.

The original Pourbaix diagrams for the three cases, generated by CorrosionAnalyzer 2.0 (Build 2.0.16) by OLI Systems Inc.,[4,5] are shown in Fig. 1. As Spahui and Puigdomenech state, the potential for the oxygen line (b) is dependent on the pH and partial pressure of O_2 following

$$E_{SHE} = 1231\ mV - 59.16\ pH + 59.16\ (\log p_{O_2})/4 \qquad [1]$$

Line (b) moves in the negative direction as the partial pressure of O_2 is decreased. Our calculations show the potential is 1.185 V(NHE) at a pH of 0 when the partial pressure of O_2 is minimized by a N_2 blanket. At a partial pressure of 0.21 atm, the potential is 1.219 V(NHE) at pH = 0. The model used to produce the (b) line is in agreement with Eq. 1.

It is important to understand the distinction between the ORP and the lines represented by the letters (a) and (b). The ORP is a mixed potential with simultaneous forward and backward components with contributions from the metal/metal ion/multiple metal ion oxidation states (e.g. Cu/Cu[I]/Cu[II], H_2/H^+, and $O_2/OH^-/H_2O$ reactions). The lines (a) and (b) describe only one half-reaction each, and, therefore, describe only a thermodynamic limit in the absence of polarization. The ORP is the potential associated with the equilibrium state between several such reactions such that the charge is balanced among all participating reactions.

The ORP of the system calculated by the OLI software includes effects of the copper metal activity as well as the partial pressures of O_2 and H_2. The ORP shown as circles in Fig. 1 includes the effects of the redox reaction required to get the solution to the stated Cu activity (1×10^{-6} M by default) and includes the influence of the generated H_2 and/or O_2. In the absence of dissolved oxygen and hydrogen, as shown in Fig. 1b, the ORP has a value of 0.403 V(NHE).

We agree with the observation of Spahiu and Puigdoimenech that the species Cu^+ identified in the upper left corner in our Pourbaix diagram was in error. As shown in Fig. 1, the correct species is $CuNO_3^+$ when using NaOH and HNO_3 as titrants.

In summary, the concerns raised by Spahiu and Puigdoimenech that the use of a single Pourbaix diagram oversimplified the thermodynamics and that a species was incorrectly labeled are justified. The calculation of the ORP in our work, however, is correct. The calculation of the ORP in the Pourbaix diagrams was used to demonstrate that, in the absence of hydrogen, copper may corrode in anoxic water. The concerns raised by Spahiu and Puigdoimenech do not invalidate the results presented in Cleveland et al.[1]

Trace Amounts of Oxygen

Our system was maintained under positive pressure with high-purity nitrogen and the oxygen content of the gas phase leaving the system was measured to be on the order of 1 ppb. The Henry's constant for this system (see Ref. 6) would suggest that, under equilibrium conditions, the dissolved oxygen concentration in water should be less than 1 ppt. Nevertheless, we appreciate that it is difficult to achieve anoxic conditions.

The main features of our experimental results are as follows:

1. Our impedance diagrams showed reactivity that was not present for gold or platinum electrodes.

*Electrochemical Society Fellow.
[z]E-mail: meo@che.ufl.e

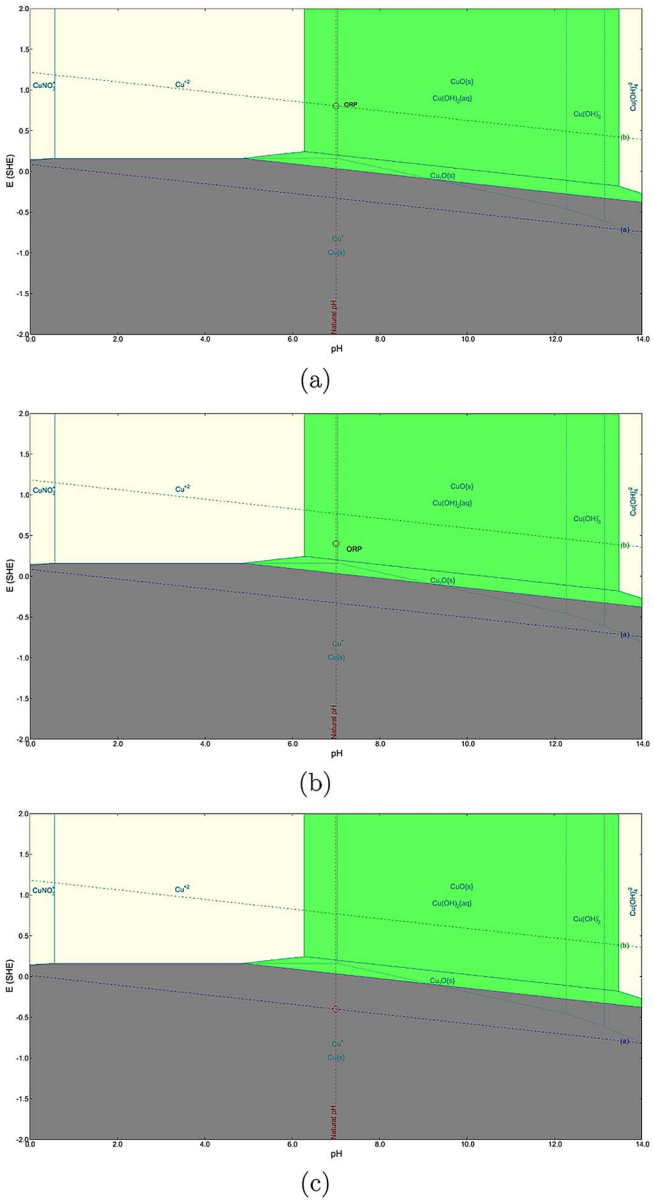

Figure 1. Calculated potential-pH (Pourbaix) diagrams for copper in deaerated deionized water generated by CorrosionAnalyzer 2.0 (Build 2.0.16) by OLI Systems Inc:[4,5] a) in the presence of 8 ppm dissolved O_2; b) in the absence of dissolved H_2 and O_2; and c) in the absence of dissolved O_2 and in the presence of dissolved H_2. The titrants were NaOH and HNO_3.

2. The impedance diagrams could not be used to extract a corrosion rate. Only an upper bound for the corrosion rate could be estimated.
3. The high-frequency part of the impedance spectrum was analyzed to show that the constant-phase element evident in the impedance response could not be attributed to an oxide film on the copper. The constant-phase element parameters were shown to be consistent with a surface distribution.

The impedance results motivated the kinetic analysis that was used to estimate a corrosion rate. The impedance was not used to quantify a corrosion rate. The absence of an oxide film and the inability to quantify a corrosion rate suggests, however, that deaeration was achieved to a high degree.

In summary, the concern on trace amounts of oxygen expressed by Spahiu and Puigdoimenech have no bearing on the conclusions drawn in our paper.

Comparison to Work of Hultquist et al.

The concern expressed by Spahiu and Puigdomenech was that our estimated corrosion rate is around three orders of magnitude higher than that derived from the observations published by Hultquist et al.[2,3] This discrepancy may be readily understood by recognizing that the approach to the equilibrium condition is governed by kinetic parameters such as rate constants, mass-transfer coefficients, and the electrode area to volume ratio. To explore the influence of system parameters, the simulations presented in our paper[1] were extended to include the oxidation of hydrogen and diffusion of dissolved hydrogen away from the electrode surface.

Mathematical development.— The reactions considered at the copper electrode were dissolution and electroplating of copper

$$Cu \rightleftarrows Cu^{2+} + 2e^- \quad [2]$$

and hydrogen evolution and oxidation

$$2H^+ + 2e^- \rightleftarrows H_2 \quad [3]$$

Kinetic parameters were taken from Stanković and Vuković[7] and Sharifi-Asla and Macdonald.[8]

The anodic current density for Reaction 2 was expressed as

$$i_{a,Cu} = i_{0,Cu} \exp(b_{a,Cu}(V - V_{0,Cu})) \quad [4]$$

where $V_{0,Cu}$ is the equilibrium potential for the copper reaction. The corresponding cathodic current density was expressed as

$$i_{c,Cu} = -\left(\frac{c_{Cu^{2+}}(0)}{c_{Cu^{2+}}(\text{ref})}\right)^{\gamma_{Cu}} i_{0,Cu} \exp\left(-b_{c,Cu}\left(V - V_{0,Cu}\right)\right) \quad [5]$$

where the concentration term $c_{Cu^{2+}}(0)$ accounts for the concentration of cupric ion at the electrode surface and $c_{Cu^{2+}}(\text{ref})$ represents the concentration of cupric ion at which the exchange current density was obtained. The anodic hydrogen oxidation in Reaction 3 was expressed as

$$i_{a,H_2} = \left(\frac{c_{H_2}(0)}{c_{H_2}(\text{ref})}\right)^{\gamma_{H_2}} i_{0,H_2} \exp\left(b_{a,H_2}\left(V - V_{0,H_2}\right)\right) \quad [6]$$

where $c_{H_2}(0)$ is the concentration of dissolved hydrogen at the electrode surface and $c_{H_2}(\text{ref})$ represents the concentration of hydrogen at which the exchange current density was obtained. The corresponding cathodic reaction was expressed as

$$i_{c,H_2} = -i_{0,Cu} \exp\left(-b_{c,H_2}\left(V - V_{0,H_2}\right)\right) \quad [7]$$

where V_{0,H_2} is the equilibrium potential for the hydrogen evolution reaction. The net rate of Reaction 2 was expressed in terms of the concentrations at the electrode surface and far from the electrode surface by

$$i_{a,Cu} + i_{c,Cu} = nFk_{Cu^{2+}}\left(c_{Cu^{2+}}(0) - c_{Cu^{2+}}(\infty)\right) \quad [8]$$

where $k_{Cu^{2+}}$ is the mass transfer coefficient for cupric ions. The net rate of Reaction 3 was expressed as

$$i_{a,H_2} + i_{c,H_2} = nFk_{H_2}(c_{H_2}(0) - c_{H_2}(\infty)) \quad [9]$$

where k_{H_2} is the mass transfer coefficient for dissolved hydrogen. The total current for the system was set equal to zero, i.e.,

$$i_{a,Cu} + i_{c,Cu} + i_{a,H_2} + i_{c,H_2} = 0 \quad [10]$$

The nonlinear set of Equations 4 through 10 were solved at each time step for variables $i_{a,Cu}$, $i_{c,Cu}$, i_{a,H_2}, i_{c,H_2}, $c_{Cu^{2+}}(0)$, $c_{H_2}(0)$, and V.

An open system is defined here to be one in which the flow of inert gas removes the hydrogen formed by Reaction 3. For an open system, the concentration of hydrogen far from the electrode at time step k was obtained from the corresponding value at time step k − 1 from

$$c^k_{H_2}(\infty) = c^{k-1}_{H_2} \quad [11]$$

As the initial hydrogen concentration was equal to zero, Eq. 11 ensured that the concentration far from the electrode was fixed to a zero value. A closed system allowed the accumulation of hydrogen. For the closed system, the concentration of hydrogen far from the electrode at time step k was obtained from the corresponding value at time step k − 1 from

$$c^{k}_{H_2}(\infty) = c^{k-1}_{H_2}(\infty) - \frac{i^{k-1}_{a,H_2} + i^{k-1}_{c,H_2}}{nF}\frac{A}{V}\Delta t \quad [12]$$

For both open and closed systems, the concentration of cupric ions far from the electrode at time step k was obtained from the corresponding value at time step k−1 from

$$c^{k}_{Cu^{2+}}(\infty) = c^{k-1}_{Cu^{2+}}(\infty) + \frac{i^{k-1}_{a,Cu} + i^{k-1}_{c,Cu}}{nF}\frac{A}{V}\Delta t \quad [13]$$

A time step of 1000 seconds was used for these simulations. For the closed system, the partial pressure of hydrogen in equilibrium with $c_{H_2}(\infty)$ was obtained using Henry's law, i.e.,

$$p_{H_2} = \frac{c_{H_2}(\infty)}{k^{o}_{H}} \quad [14]$$

where $k^{\circ}_{H} = 0.00078$ mol/kg bar.[6]

Mass-transfer coefficients.— Mass–transfer coefficients were obtained from published correlations for the microelectrode used in our work[1] and the copper foils used in the work by Hultquist et al.[2] The relationship between the mass–transfer coefficient for cupric ions and dissolved hydrogen differed for the two cases because transport for the microelectrode was assumed to be controlled by diffusion and transport for the foils was assumed to be controlled by natural convection.

Microelectrode.—For the microelectrode considered in our work, the mass-transfer coefficient was obtained from the expression[9]

$$Sh_i = \frac{k_i d_{disk}}{D_i} = \frac{8}{\pi} \quad [15]$$

where Sh_i is the dimensionless Sherwood number, k_i is the mass transfer coefficient of species i, d_{disk} is the diameter of the disk, and D_i is the diffusivity of species i. The mass transport represented in Eq. 15 is mathematically equivalent to spherical diffusion for a microelectrode. Thus, the mass transfer coefficients for cupric ions and dissolved hydrogen were related by

$$k_{H_2} = k_{Cu^{2+}}\frac{D_{H_2}}{D_{Cu^{2+}}} \quad [16]$$

The electrode diameter was 0.025 cm and the volume of water was 30 cm^3 yielding an area to volume ratio of $A/V = 1.64 \times 10^{-5}$ cm^{-1}. From Eq. 15, the mass transfer coefficient for cupric ions can be estimated to have a value of $k_{Cu^{2+}} = 7.33 \times 10^{-4}$ cm/s.

Hultquist foils.—The experimental systems reported by Hultquist et al.[2] consisted of copper foils with an exposed area of 85 cm^2 placed upright in a sealed vessel and immersed in anoxic water with a volume of 50 cm^3. Such a system may be expected to be driven by natural convection. A correlation for natural convection to a vertical plate is given as[10]

$$Sh_i = \frac{k_i L}{D_i} = 0.677\,(Sc\,Gr)^{1/4} \quad [17]$$

where L is the length of the plate, $Sc = \nu/D_i$ is the Schmidt number, and ν is the kinematic viscosity of the electrolyte. The term Gr is the Grashof number defined for $\rho(0) > \rho(\infty)$ as

$$Gr = \frac{gL^3}{\nu^2}\left(1 - \frac{\rho(\infty)}{\rho(0)}\right) \quad [18]$$

where g is gravitational acceleration, ν represents the average electrolyte kinematic viscosity, $\rho(\infty)$ is the electrolyte density far from the electrode, and $\rho(0)$ is the electrolyte density at the electrode surface.

Table I. Kinetic parameters used for the numerical simulations. Mass–transfer coefficients used in the simulations are presented as legends in the respective figures. Values for the equilibrium potential for the copper dissolution reaction were taken from Figure 1 of Ref. 7 and adjusted to be referenced to the Normal Hydrogen Electrode. The kinetic parameters for the hydrogen evolution reaction were taken from Ref. 8 for pH = 0 and p_{H_2} = 0.1 atm. See Table III in Cleveland et al.[1]

Parameter	Value	Units
$V_{0,Cu}$	−0.1876	V(NHE)
$i_{0,Cu}$	9×10^{-4}	A/cm^2
$b_{a,Cu}$	20	1/V
$b_{c,Cu}$	53.56	1/V
γ_{Cu}	0.75	
V_{0,H_2}	−0.436	V(NHE)
i_{0,H_2}	3.28×10^{-7}	A/cm^2
b_{a,H_2}	38.38	1/V
b_{c,H_2}	24.24	1/V
γ_{H_2}	1	

Thus, for a system controlled by natural convection, the mass transfer coefficients for cupric ions and dissolved hydrogen were related by

$$k_{H_2} = k_{Cu^{2+}}\left(\frac{D_{H_2}}{D_{Cu^{2+}}}\right)^{3/4} \quad [19]$$

The electrode area to volume ratio was $A/V = 1.7$ cm^{-1}. Under the assumption that the dimensionless density difference $1 - \rho(\infty)/\rho(0)$ is on the order of 10^{-9}, the mass transfer coefficient for cupric ions can be estimated to have a value of $k_{Cu^{2+}} = 1 \times 10^{-5}$ cm/s.

Results.— The calculated results are presented for both open and closed systems. In the open system, hydrogen is removed by the flow of inert gas such that the bulk concentration of dissolved hydrogen may be assumed to be equal to zero. In the closed system, the accumulation of hydrogen results in the buildup of hydrogen partial pressure. Parameters used in the simulation are presented in Table I.

Open system.—The corrosion rate calculated for the microelectrode is compared to that obtained for the Hultquist cell in Fig. 2 with mass–transfer coefficient as a parameter. For both the microelectrode and the Hultquist cell, results are presented as well for mass–transfer coefficients that are an order of magnitude larger and smaller than the corresponding calculated value. The calculated corrosion rate for the microelectrode was 1.1 nm/day and reached a value of 0.74 nm/day after 15 years; whereas, for the Hultquist cell, the calculated corrosion rate was initially about 0.37 nm/day and reached a value of 0.053 nm/day after 15.2 years. The corrosion rate is shown to depend on the electrode area to volume ratio and on the mass–transfer coefficients.

The cumulative corrosion is presented as a function of time in Fig. 3 for the microelectrode and Hultquist cells. After an elapsed time of 15 years, the cumulative corrosion for the microelectrode was estimated to be 4700 nm; whereas, the cumulative corrosion for the Hultquist cell was calculated to be 390 nm. Thus, using the same model for the kinetics, the calculation for cumulative corrosion that accounted for mass transfer and the electrode area to volume ratio yielded a cumulative corrosion for the microelectrode that was 12 times larger than for the Hultquist cell.

The influence of electrode area to volume ratio is evident in the concentration of cupric ion presented in Fig. 4 for the microelectrode and Hultquist cells. The calculated bulk concentration of cupric ion reached a value of 9.3 μmol/cm^3 after 15 years in the Hultquist cell. In contrast, the calculated bulk concentration of cupric ion for the microelectrode reached a value of 1.0 nmol/cm^3 after 15 years in the Hultquist cell, which is 10,000 times smaller than that obtained for the Hultquist cell. The difference can be attributed to the different electrode area to volume ratios and to the difference in mass–transfer coefficients. For the open system, the bulk concentration of dissolved

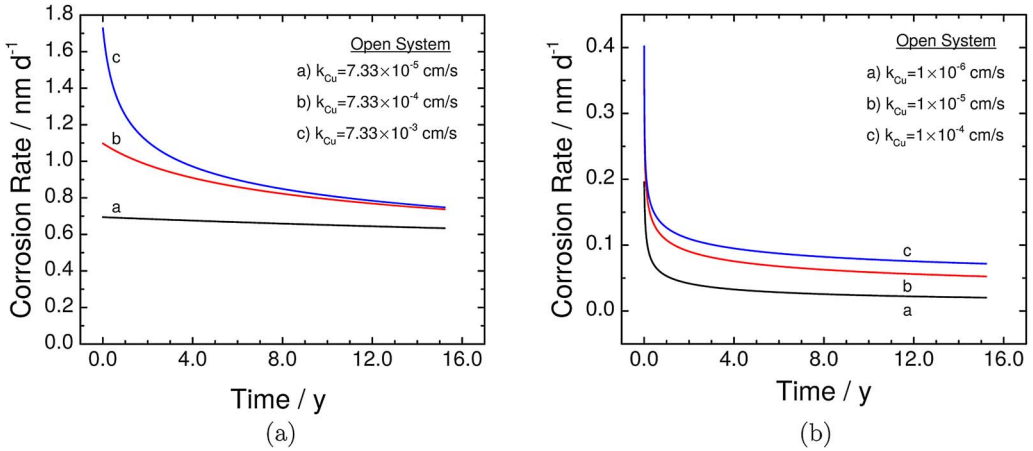

Figure 2. Calculated open–system corrosion rates as a function of time with mass–transfer coefficient as a parameter: a) for the microelectrode with $A/V = 1.64 \times 10^{-5}$ cm^{-1}; b) for the Hultquist cell with $A/V = 1.7$ cm^{-1}.

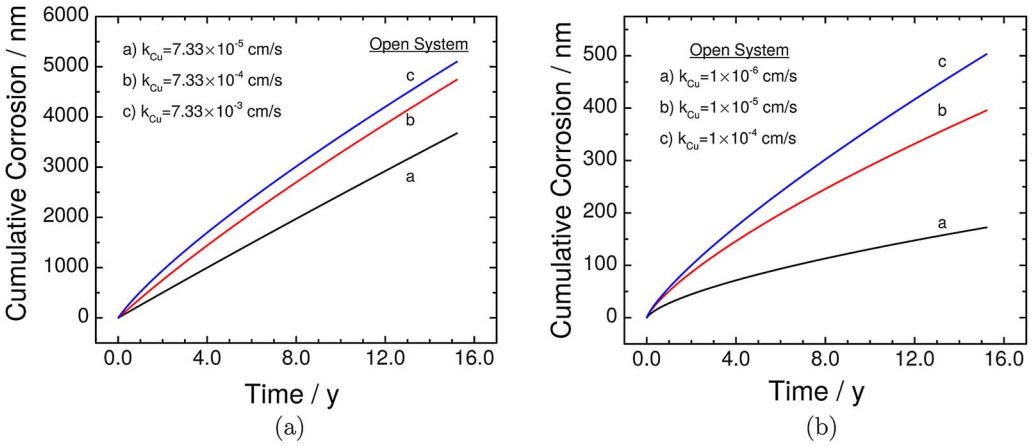

Figure 3. Calculated open–system cumulative corrosion as a function of time with mass–transfer coefficient as a parameter: a) for the microelectrode with $A/V = 1.64 \times 10^{-5}$ cm^{-1}; b) for the Hultquist cell with $A/V = 1.7$ cm^{-1}.

hydrogen was assumed to be equal to zero. Thus, the corrosion continues in both the microelectrode and Hultquist systems, even after a period of 15 years.

Closed system.—The behavior of an open system may be expected to differ from that of a closed system, in which the concentration of dissolved hydrogen and the corresponding hydrogen partial pressure increases with time. The closed–system corrosion rate calculated for the microelectrode is compared to that obtained for the Hultquist cell in Fig. 5 with mass–transfer coefficient as a parameter. For both the microelectrode and the Hultquist cell, results are presented as well

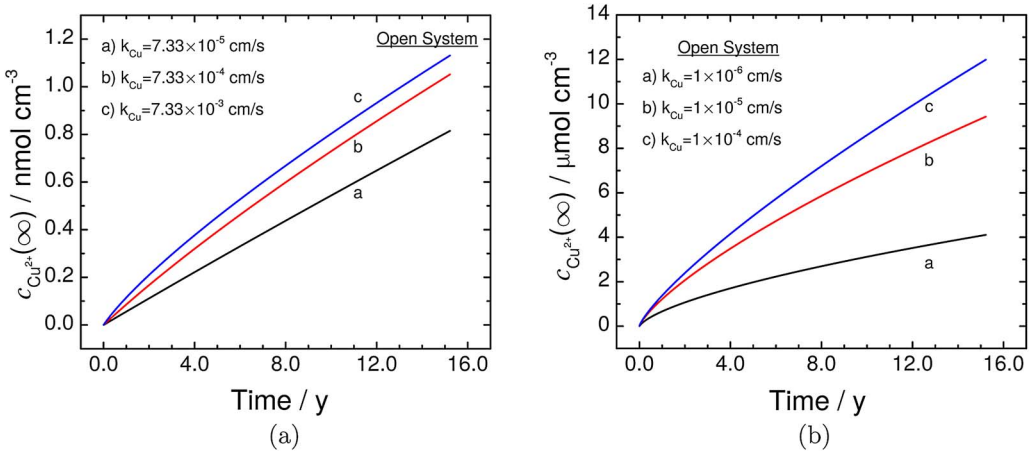

Figure 4. Calculated open–system bulk concentration of cupric ion as a function of time with mass–transfer coefficient as a parameter: a) for the microelectrode

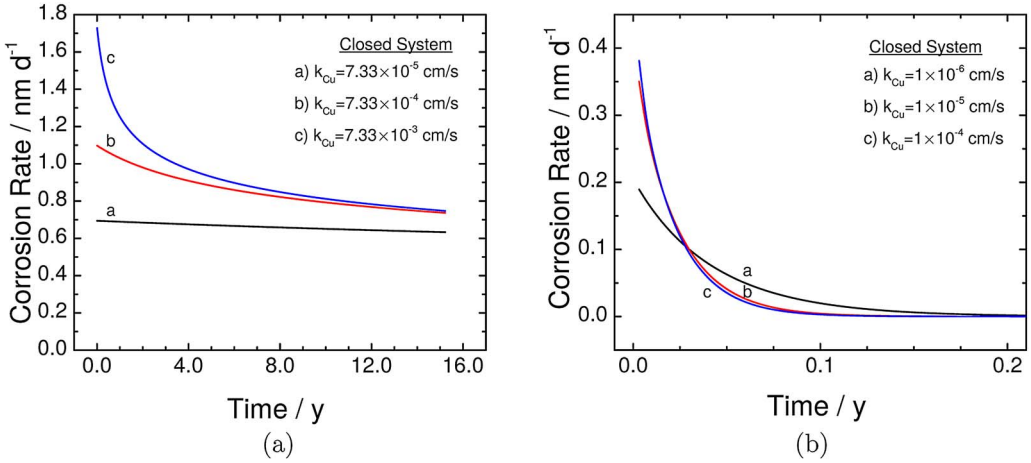

Figure 5. Calculated closed–system corrosion rates as a function of time with mass–transfer coefficient as a parameter: a) for the microelectrode with $A/V = 1.64 \times 10^{-5}$ cm^{-1}; b) for the Hultquist cell with $A/V = 1.7$ cm^{-1}.

for mass–transfer coefficients that are an order of magnitude larger and smaller than the corresponding calculated value. The calculated corrosion rate for the microelectrode was 1.1 nm/day and reached a value of 0.74 nm/day after 15 years, essentially unchanged from the results of the open system shown in Fig. 2a. In contrast, the corrosion rate calculated for the Hultquist cell was initially about 0.35 nm/day and dropped to a value near zero in less than 60 days. The insensitivity to the open or closed condition for the microelectrode may be attributed to the small electrode area to volume ratio. The sharp decrease in the corrosion rate in the closed Hultquist cell can be attributed to the larger electrode area to volume ratio.

The corresponding cumulative corrosion is presented as a function of time in Fig. 6 for the microelectrode and Hultquist cells. After an elapsed time of 15 years, the cumulative corrosion for the closed–system microelectrode was unchanged from that in the open system; whereas, the cumulative corrosion for the Hultquist cell was calculated to be 2.7 nm. Thus, using the same model for the kinetics, the calculation for cumulative corrosion that accounted for mass transfer and the electrode area to volume ratio yielded a cumulative corrosion for the microelectrode that was 1700 times larger than for the Hultquist cell.

The influence of electrode area to volume ratio is evident in the concentration of cupric ion presented in Fig. 7 for the microelectrode and Hultquist cells. The calculated bulk concentration of cupric ion in the Hultquist cell reached a value of 75 nmol/cm^3, much smaller than the 9.3 μmol/cm^3 reached in the open system after 15 years. In contrast, the calculated bulk concentration of cupric ion for the microelectrode after 15 years was unchanged as compared to the open system. The difference in behavior between the microelectrode and Hultquist systems is due to the difference in electrode area to volume ratio.

The major difference between the open and closed system is that the hydrogen partial pressure is allowed to increase in a closed system. The hydrogen partial pressure, calculated from the bulk concentration of dissolved hydrogen, is presented in Fig. 8 as a function of time for the microelectrode and Hultquist cells. The Henry's law constant used for this calculation were obtained from Sander.[6] After less than 60 days, the calculated closed–system hydrogen partial pressure reached a limiting value of 0.096 atm; whereas, in the closed microelectrode system, the hydrogen partial pressure did not reach a limiting value and, after 15 years, reached a value of 0.0013 atm. The limiting value of hydrogen partial pressure was found to be independent of mass–transfer coefficient and exchange current density, but did depend on the equilibrium potential used.

A clearer understanding of the calculations performed in the present work may be obtained from the calculated corrosion current–potential relationship presented in Fig. 9 for the Hultquist cell under open and closed condition. For the closed system, the corrosion current density approaches a value of zero at a potential of −0.284 V(NHE). This value is independent of mass–transfer

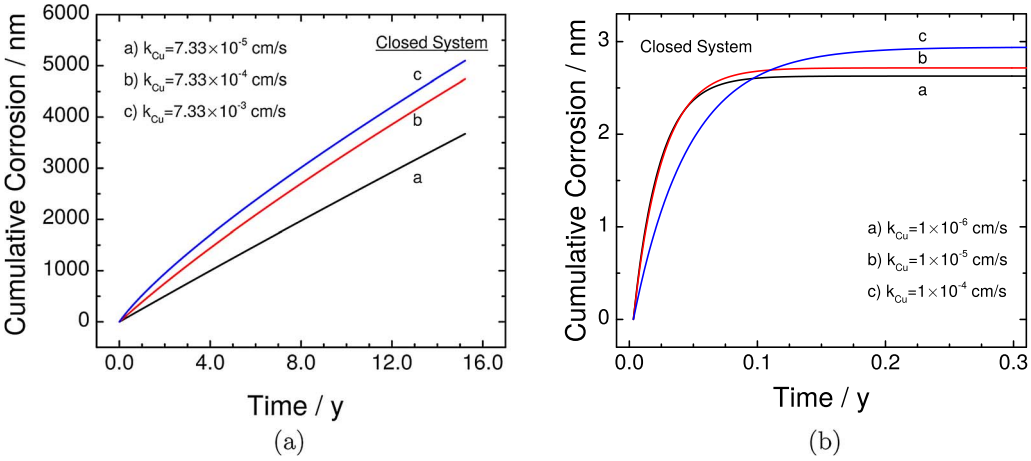

Figure 6. Calculated closed–system cumulative corrosion as a function of time with mass–transfer coefficient as a parameter: a) for the microelectrode with

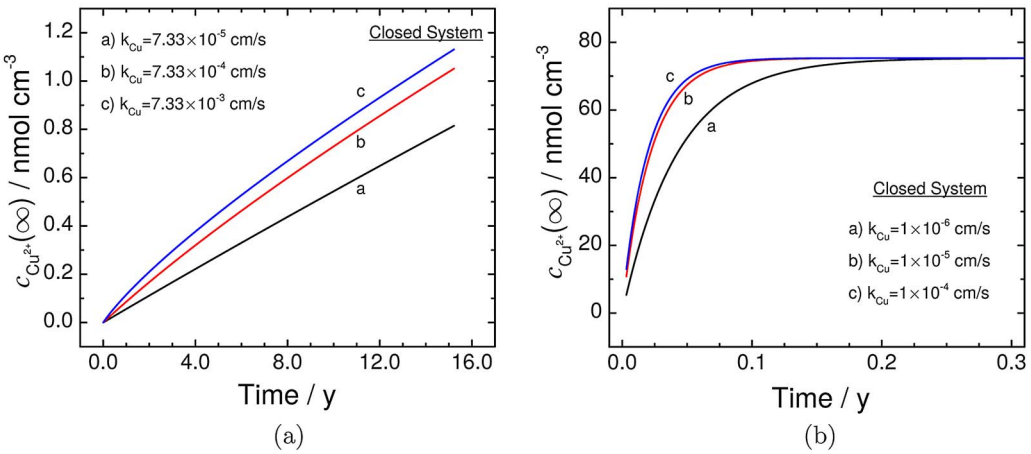

Figure 7. Calculated closed–system bulk concentration of cupric ion as a function of time with mass–transfer coefficient as a parameter: a) for the microelectrode with $A/V = 1.64 \times 10^{-5}$ cm^{-1}; b) for the Hultquist cell with $A/V = 1.7$ cm^{-1}.

coefficient and is in good agreement with the Pourbaix diagrams presented in Fig. 1. For the open system, the corrosion current density decreases as the potential increases. The equilibrium condition is not achieved as the accumulation of hydrogen is prevented. The calculated limiting hydrogen partial pressure of 0.096 atm is substantially larger than the value of 0.45 mbar reported by Hultquist et al.[3] In addition, the corrosion rate estimated in the present work for the Hultquist system is smaller than the rate reported by Hultquist et al.[3] This discrepancy may be attributed to experimental issues or to the need to modify the model parameters. The model reported in the present work did not account for the contribution of the head space. The hydrogen pressure was assumed to be that in equilibrium with the bulk concentration of dissolved hydrogen. Thus, the measured hydrogen pressure may be expected to be lower than that calculated. The presence of a large head space would cause the system to behave as an open system at short times and as a closed system as the partial pressure of hydrogen increases in the head space. The agreement between the simulations performed in the present work to those presented in Cleveland et al.[1] validate the assumption made that the hydrogen oxidation reaction could be neglected for the small electrode area to volume ratio and short times considered. The hydrogen oxidation reaction plays an essential role in simulating the behavior of the Hultquist cell with its larger electrode area to volume ratio and experiments of longer duration. For both the open and closed systems, the cumulative corrosion is reduced for larger electrode area to volume ratios.

The difference in estimated corrosion rates between our work[1] and that Hultquist et al.[2] is shown in the present work to be the natural consequence of the manner in which kinetics, mass transfer, and electrode area to volume ratio influence the progression toward the equilibrium condition. The concerns raised by Spahiu and Puigdoimenech do not invalidate the conclusions presented in Cleveland et al.[1]

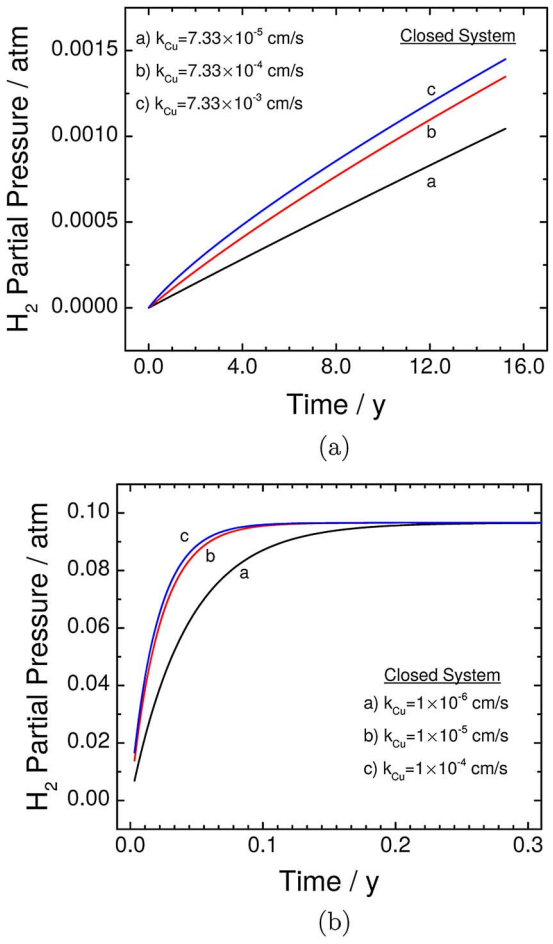

Figure 8. Calculated closed–system bulk hydrogen partial pressure as a function of time with mass–transfer coefficient as a parameter: a) for the microelectrode with $A/V = 1.64 \times 10^{-5}$ cm^{-1}; b) for the Hultquist cell with $A/V = 1.7$ cm^{-1}.

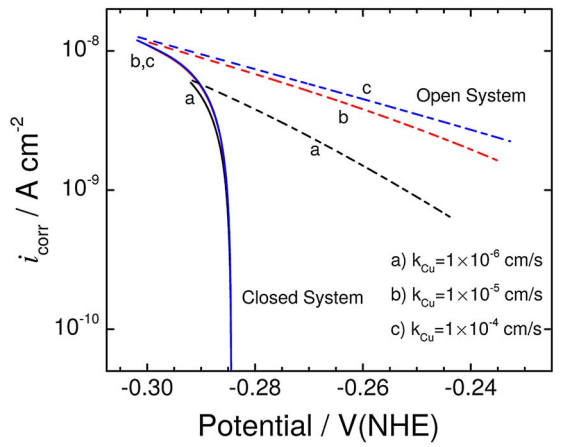

Figure 9. Calculated corrosion current density as a function of potential for the Hultquist cell under open and closed condition with mass–transfer coefficient as a parameter.

Conclusions

We consider the comment on the thermodynamic analysis to be justified in the sense that, while our thermodynamic analysis was correct, it could have been presented more clearly. The comment on the possible presence of oxygen in our experiments does not influence the conclusion of our paper as our conclusion was based on simulation results using parameters extracted from the literature. The impedance results were used only to show that an oxide film was not present on the copper electrode and to provide an upper bound for the corrosion rate of 2.5 nm/day. The comment that the difference in estimated corrosion rates between our system and that of Hultquist somehow invalidates our results is shown in the present work to be without basis. The difference in estimated corrosion rates is the natural consequence of scale and transport differences between the two systems.

Acknowledgments

The authors gratefully acknowledge the contributions of Dr. Douglas P. Riemer in the preparation of this response.

References

1. C. Cleveland, S. Moghaddam, and M. E. Orazem, "Nanometer-Scale Corrosion of Copper in De-Aerated Deionized Water," *J. Electrochem. Soc.*, **161**, C107 (2014).
2. G. Hultquist, P. Szakálos, M. J. Graham, G. I. Sproule, and G. Wikmark, "Detection of Hydrogen in Corrosion of Copper in Pure Water," in *Proceedings of the 2008 International Corrosion Congress*, Paper 3884, p. 1 (2008).
3. G. Hultquist, M. J. Graham, O. Kodra, S. Moisa, R. Liu, U. Bexell, and J. L. Smialek, "Corrosion of Copper in Distilled Water without O_2 and the Detection of Produced Hydrogen," *Corros. Sci.*, **95**, 162 (2015).
4. A. Anderko and P. J. Shuler, "A Computational Approach to Predicting the Formation of Iron Sulfide Species Using Stability Diagrams," *Comput. Geosci.*, **23**, 647 (1997).
5. A. Anderko, S. J. Sanders, and R. D. Young, "Real Solution Stability Diagrams: A Thermodynamic Tool for Modeling Corrosion in Wide Temperature and Concentration Ranges," *Corrosion*, **53**, 43 (1997).
6. R. Sander, "Henry's Law Constants," in *NIST Chemistry WebBook, NIST Standard Reference Database Number 69*, P. Linstrom and W. Mallard, , Editors, National Institute of Standards and Technology, Gaithersburg MD: National Institute of Standards and Technology, http://webbook.nist.gov. Retrieved November 4, 2015.
7. Z. D. Stanković and M. Vuković, , "The Influence of Thiourea On Kinetic Parameters on the Cathodic and Anodic Reaction at Different Metals in H_2SO_4 Solution," *Electrochim. Acta*, **41**, 2529 (1996).
8. S. Sharifi-Asla and D. D. Macdonald, "Investigation of the Kinetics and Mechanism of the Hydrogen Evolution Reaction on Copper," *J. Electrochem. Soc.*, **160**, H382 (2013).
9. H. C. Hottel, J. J. Noble, A. F. Sarofim, G. D. Sikox, P. C. Wankat, and K. S. Knaebel, "Heat and Mass Transfer," in *Perry's Chemical Engineers' Handbook*, D. W. Green and R. H. Perry, Editors, 8th ed., 5:1-5:84, McGraw Hill, New York, NY (2007).
10. C. R. Wilke, M. Eisenberg, and C. W. Tobias, "Correlation of Limiting Currents under Free Convection Conditions," *J. Electrochem. Soc.*, **100**, 513 (1953).